THE OHIO STATE UNIVERSITY

DEDICATION: Mike Seaton & Dimitri Mihalas

The Renewed Opacity Project: Interface of Atomic Physics, Equation-of-state, and Astrophysical opacities

Anil Pradhan

Solar Workshop: The future of solar modeling

Geneva, September 4-7, 2023

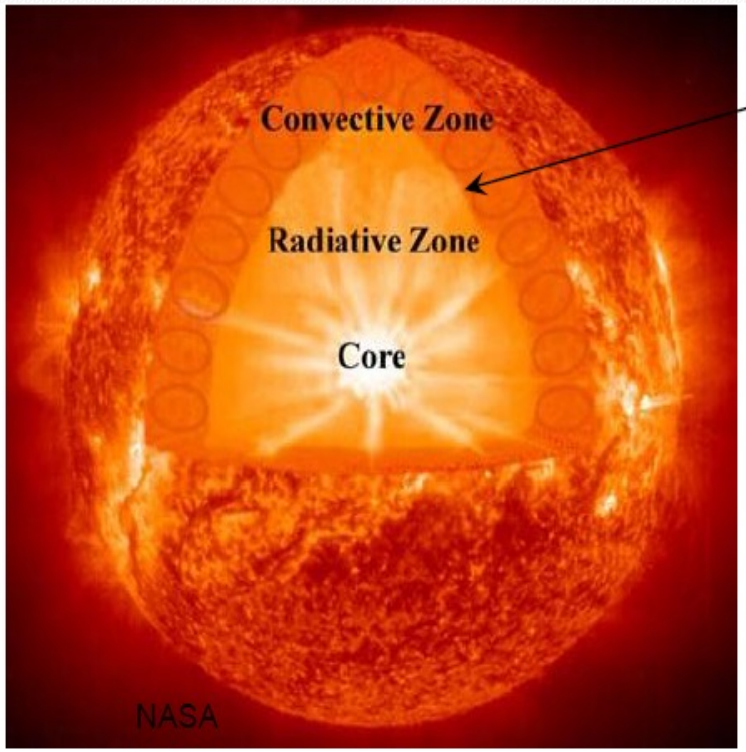

BCZ

Atomic Physics → Current: Distorted Wave
→ New: R-Matrix

Plasma Physics → Spectral broadening
→ Equation-of-state

Astrophysics → Opacities, Abundances

Why Renewed Opacity Project?

- Opacity Problem → solar abundances anomaly
- 3D NLTE models, helioseismology
- OP opacities underestimate by up to x 2
- Atomic physics issues:
  - Distorted Wave vs. R-matrix method
  - Plasma effects: resonance vs. line broadening
- Iron opacity → theory vs. expt (Fe, Cr, Ni)
- Equation-of-state issues (MHD, QMHD)

R-matrix Calculations for Opacities: I.- IV. (astro-ph and submitted)

- R-matrix Calculations for Opacities: I. Methodology and Computations (Pradhan, Nahar, Eissner) http://arxiv.org/abs/2308.14882
- R-matrix Calculations for Opacities: II. Photoionization and oscillator strengths of iron ions Fe XVII, Fe XVIII and Fe XIX (Nahar, Zhao, Eissner, Pradhan) http://arxiv.org/abs/2308.14854
- R-matrix Calculations for Opacities: III. Plasma broadening of autoionizing resonances (Pradhan) http://arxiv.org/abs/2308.14870
- R-matrix Calculations for Opacities: IV. Convergence, completeness and comparison of relativistic R-matrix and distorted wave calculations for Fe XVII and Fe XVIII (Zhao, Nahar, Pradhan) http://arxiv.org/abs/2308.14880
- Accurate R-matrix data differ considerably from the simpler Distorted Wave method used in existing opacity models, contrary to recent work by Delahaye et al. (2021) which is also incomplete (e.g. resonance broadening is not considered, RMOs not reported, cross sections not compared, etc.)

BCZ Ionization Fractions: O, Ne, Fe

Table 2. Main solar BCZ atomic opacity contributing elements and ionization states and fractions >0.03 at T = 2.24 x 10^6K and N_e = $10^{23} cm^{-3}$ obtained from [15] using the Q-form of the MHD-EOS [7, 8]. The actual opacity contribution depends significantly on the theoretical model employed with respect to solar abundances and the EOS.

Element	Ionization state (fraction)
Oxygen	O VII (0.11) O VIII (0.47) O IX (0.42)
Neon	Ne VIII (0.10) Ne IX (0.51) Ne X (0.35)
Iron	Fe XVI (0.08) Fe XVII (0.30) Fe XVIII (0.37) Fe XIX (0.18) Fe XX (0.04)

- Atomic Ions and fractions at BCZ for dominant Elements and opacities
- O, Ne data for H-He-Li-like ions likely same in all models
- Fe most likely discrepant (Bailey et al., Nature 2015; Nahar and Pradhan, PRL 2016)

← Fully ionized, H-like, He-like

H-Li-like ←

← Na-,Ne-.F-,O-,N-like L-shell electrons

New Atomic-Plasma Opacities

- The Opacity Project (OP): Atomic data for opacities (1983-2007):
  Seaton, Mihalas, Burke, Hummer, Dappen, et al. → OPCD, OPSERVER
- R-Matrix (RM) methodology for bound-free photoionization cross sections and bound-bound transition probabilities
- But RM calculations proved intractable due to inner-shell transitions
- OPCD: mainly Distorted Wave (DW) as other opacity models
- **Renewed** OP: Fine structure via Breit-Pauli RM (BPRM) method
- BPRM opacities calculations with channel couplings, viz. manifest in **autoionization resonances** in bound-free continua
- New versions of codes for atomic data, equation-of-state, & opacities
- First results for Fe XVII RM opacities (Nahar and Pradhan 2016)
- Atomic-plasma physics criteria for accuracy of opacity calculations
  -- Convergence of coupled channel BPRM calculations
  -- Completeness including all contributing configurations
  -- Plasma broadening of autoionizing resonances

R-Matrix (RMOP) Codes and Data

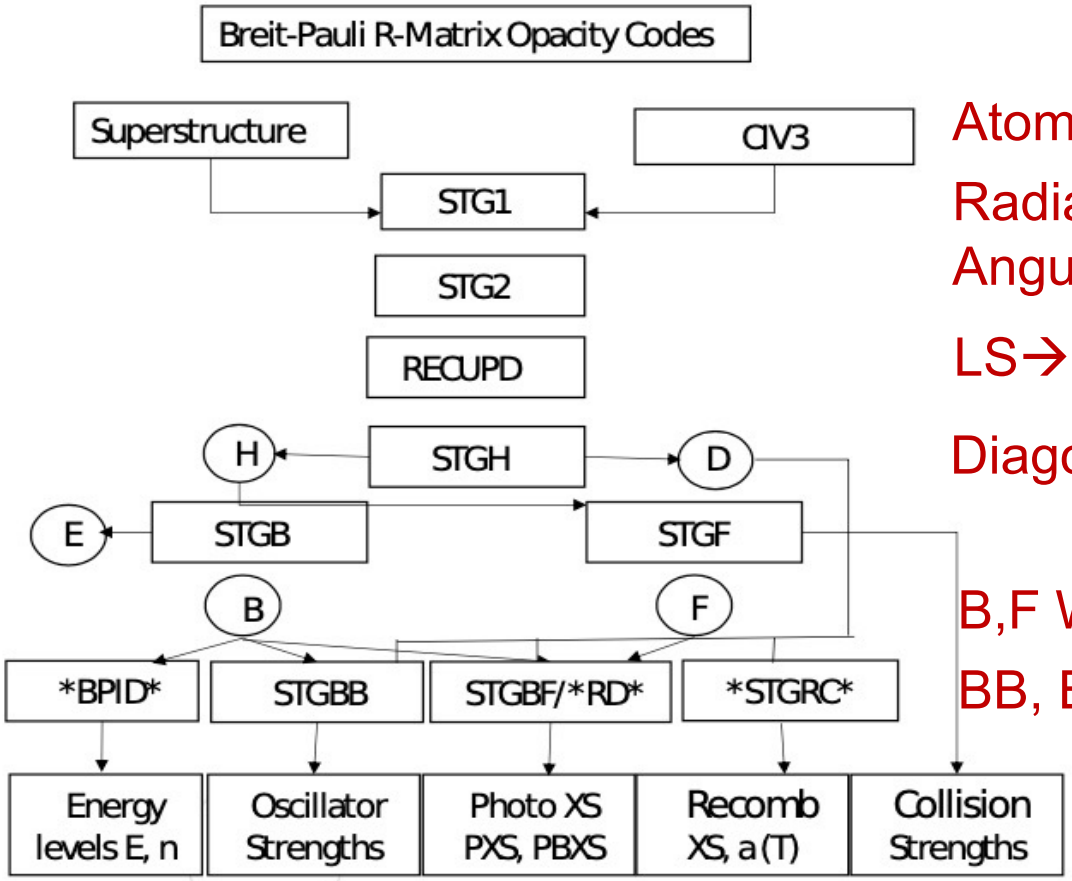

Atomic Structure

Radial Integrals
Angular Algebra

LS→J Recoupling

Diagonalization

B,F Wavefunctions

BB, BF, Recomb

New Opacity Codes

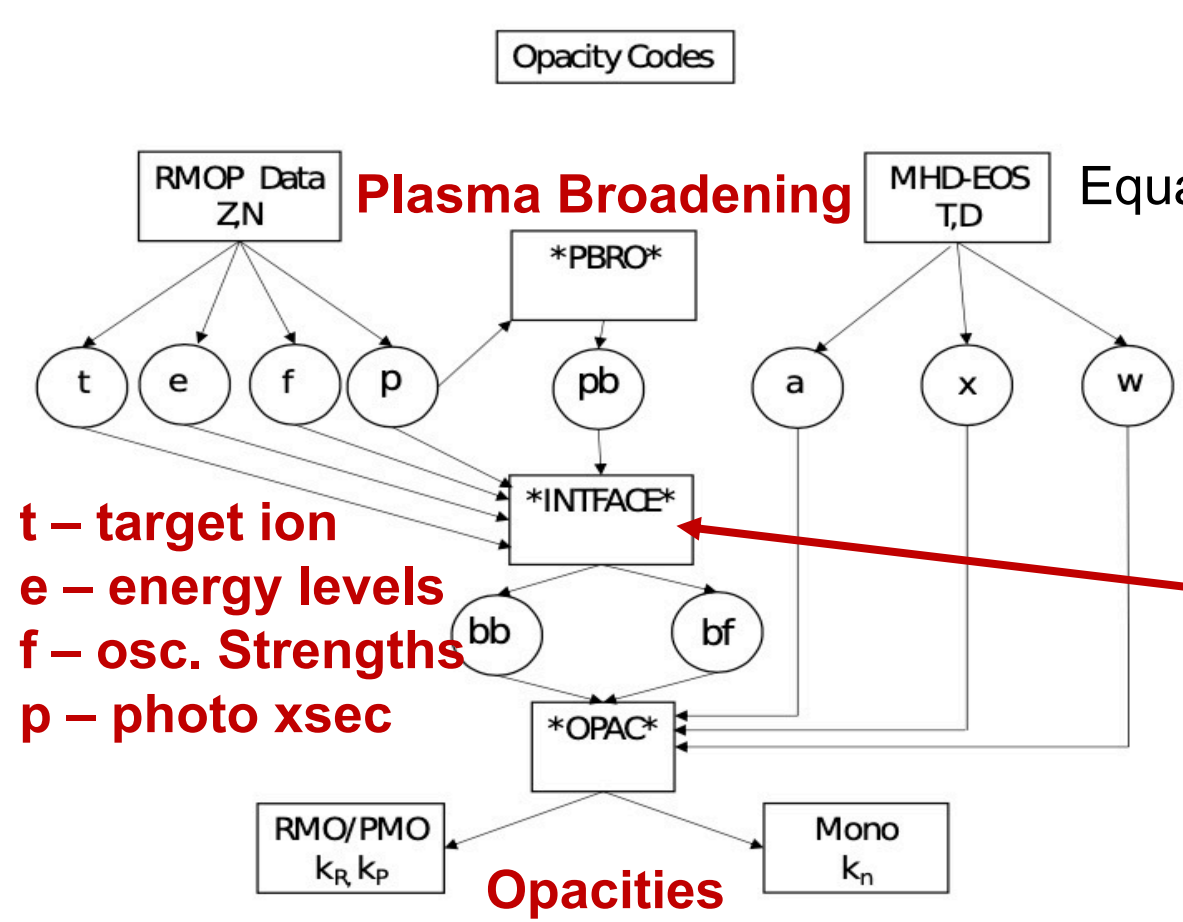

t – target ion
e – energy levels
f – osc. Strengths
p – photo xsec

a – abundances
x – ion fractions
w – occupation prob.

Interface and Map atomic data on 10^5 $h\nu/kT$ mesh

Atomic Processes in Plasmas: Unified R-Matrix Methodology

(Pradhan and Nahar, "Atomic Astrophysics and Spectroscopy", Cambridge 2011)

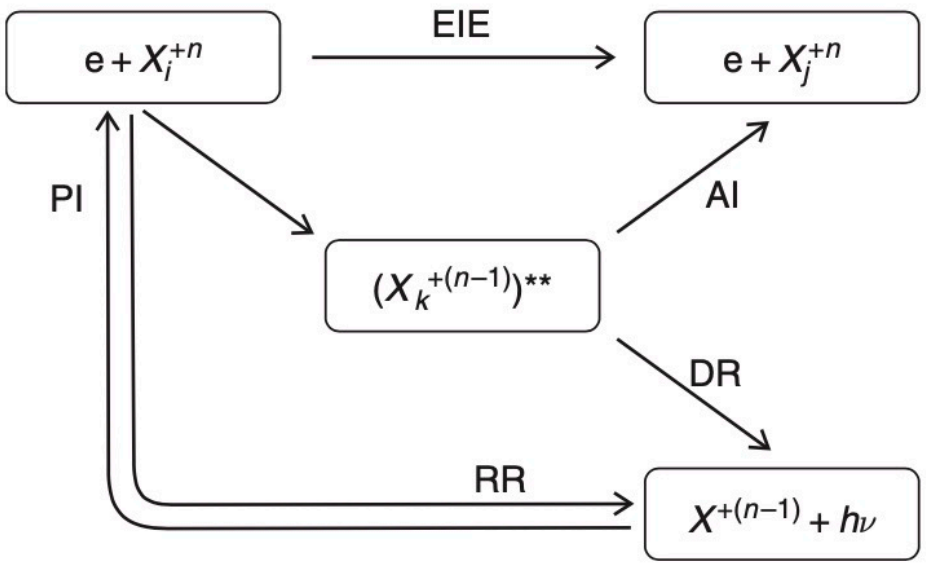

FIGURE 3.5 Unified picture of dominant atomic processes in plasmas: electron impact excitation (EIE), photoionzation (PI), autoionization (AI), dielectronic recombination (DR) and radiative recombination (RR). Note the often important role of resonance states in the centre, mediating atomic processes.

R-matrix method may be used for all these processes with the same wavefunction expansion for bound and Continuum states of an (e+ion) System in a unified and self-consistent manner ensuring uniform accuracy

Electron-ion wavefunction

(N+1) electron system: N-electron ion and free electron

$$\Psi = \mathcal{A}\left[\sum_{i}^{n_f} \Phi_i(x_1, \ldots x_N)\, \frac{1}{r} F_i(r)\right]$$

- **Ion wavefunctions from atomic structure codes: Superstructure, CIV3, GRASP**
- **$F_i(r)$ to be determined using RM**

A – antisymmetrization operator → Exchange effect

E < 0 → -ve energy state of (N+1) electron system with 'free' electron bound
E > 0 → +ve energy with 'free' electron in continuum or free state
Example: (Fe XVIII + e) → Fe XVII

Resonances: Bound and continuum states

(R-matrix method: Coupled wavefunctions)

Uncoupled bound states

$$\Psi_i \rightarrow |<\Psi_j \| D \| \Psi_i>|^2 \rightarrow$$

Symmetric line profile

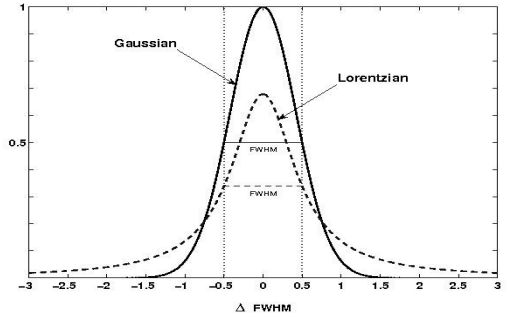

Coupled bound and continuum states

Autoionization

$$\sum_i \Psi_i \rightarrow |<\sum_j \Psi_j \| D \| \sum_i \Psi_i>|^2 \rightarrow$$

Asymmetric resonance profile

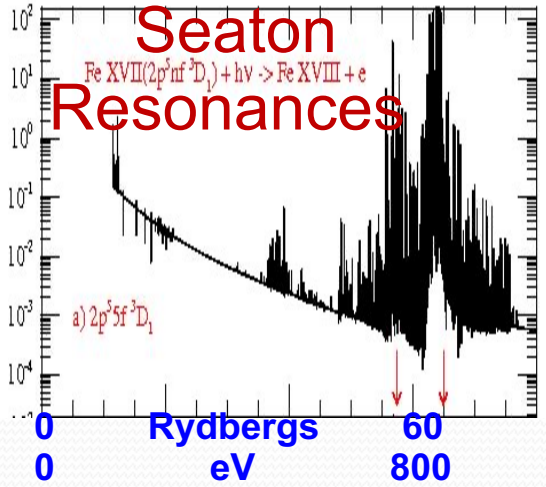

$\sum\int$ **Coupled channel approximation**

Distorted Wave Approximation neglects autoionization ab initio

R-matrix calculations for opacities. III. Coupled channels and autoionizing (AI) resonances

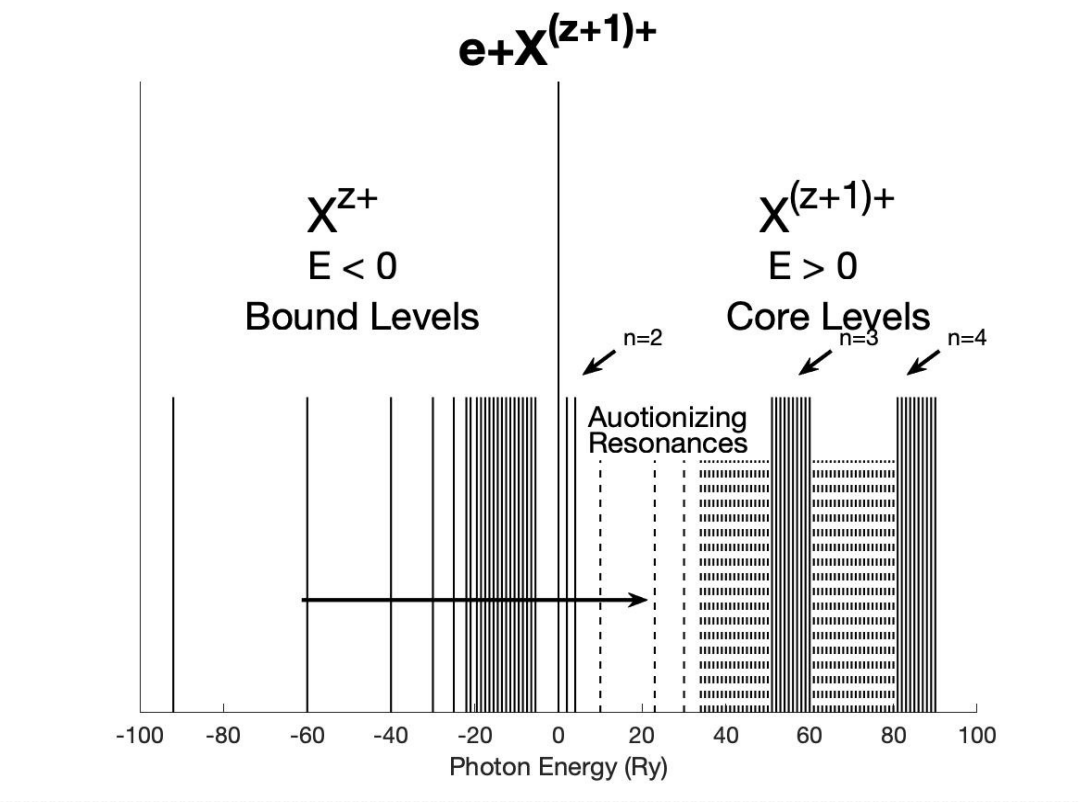

- **Photoionization**

With AI resonances

- **X^{z+1} nl – bound levels**
  E < 0
- **X^{z+1} εl – continuum**

E > 0, free electron energy ε

- **AI levels:**

X^{z+1} nl ←→ X^{z+1} εl

$$E(n\ell) = \frac{z^2}{(n-\mu)^2}. \qquad (2.64)$$

Opacity

2. Monochromatic and mean opacities

The atomic parameters comprising the monochromatic opacity are due to bb, bf, free–free (ff), and photon scattering (sc) contributions:

$$\kappa_{ijk}(\nu) = \sum_k a_k \sum_j x_j \sum_{i,i'} [\kappa_{bb(}(i,i';\nu) + \kappa_{bf}(i,\epsilon i';\nu) + \kappa_{ff}(\epsilon i,\epsilon' i';\nu) + \kappa_{sc}(\nu)] \quad (1)$$

where a_k is the abundance of element k, x_j the j ionization fraction, i and i' are the initial bound and final bound/continuum states of the atomic species, and ϵ represents the electron energy in the continuum. The atomic absorption coefficients are related to the local radiation field at temperature T described by the Planck function

$$B_\nu(T) = \frac{(2h\nu^3/c^2)}{e^{h\nu/kT} - 1}. \quad (2)$$

Macrosopic quantities such as radiative forces and fluxes may be computed in terms of mean opacities, such as the Plank Mean Opacity (PMO)

$$\kappa_P B(T) = \int \kappa_\nu B_\nu d\nu. \quad (3)$$

Of particular interest to opacity calculations is the Rosseland Mean Opacity (RMO), κ_R RMO defined as the *harmonic mean* of monochromatic opacity $\kappa_{ijk}(\nu)$ as

$$\frac{1}{\kappa_R} = \frac{\int_0^\infty g(u)\kappa_\nu^{-1} du}{\int_0^\infty g(u) du} \quad ; \quad g(u) = u^4 e^{-u}(1 - e^{-u})^{-2}, \quad (4)$$

where $g(u) = dB_\nu/dT$ is the derivative of the Planck weighting function (corrected for stimulated emission). Eq. 4 is matehmatically and physically a complex quantity to

Monochromatic plasma opacity κ_ν largely depends on radiation absorption through bound-bound (bb) photo-excitation and bound-free (bf) photoionization as follows:

$$\kappa_\nu^{bb}(i \rightarrow j) = \frac{\pi e^2}{mc} N_i f_{ij} \phi_\nu; \quad \kappa_\nu^{bf} = N_i \sigma_{PI}(\nu) \qquad (1)$$

$$< f >_{\Delta E} = \sum_k^\infty \int_{\epsilon=E_k}^\infty \frac{df_{ik}}{d\epsilon} d\epsilon,$$

Integrated oscillator strength with discrete photoionized continua into excited core levels k

Explicitly including successive core excitations in σ_{PI}

$$< f >_{\Delta E} = \frac{1}{4\pi\alpha a_o^2} \sum_{E_1(k)}^{E_{n'}} \int_{\epsilon \geq E_k}^\infty \sigma_{ik} d\epsilon_k,$$

Large-scale photoionization calculations into many excited high-n cores until convergence with respect to final levels of the residual ion

Atomic Physics Methods for Opacities

- **Simple - Distorted Wave (DW):** All current opacity models employ variants of DW approximation of comparable (in)accuracy

  - DW → Atomic structure + continuum

  - no continuum channel coupling or autoionization in photoionization

  - OP: primarily Autostructure inner-shell + limited outer-shell R-Matrix

- **Complex - R-Matrix (RM):**

  - Powerful and state-of-the art, much higher accuracy than DW

  - Coupled-channel approximation

  → Electron-ion excitation, recombination, photoionization, f-values

  → extensive autoionization structure in bound-free opacity

  → **different plasma broadening effects on opacities than on bound-bound lines**

Mihalas-Hummer-Dappen Equation-of-state (MHD-EOS)

w – Level Occupation Probability

The modified Saha–Boltzmann equation is based on the concept of *occupation probability* w of an atomic level being populated, taking into account perturbations of energy levels by the plasma environment. We rewrite

$$N_{ij} = \frac{N_j g_{ij} w_{ij} e^{(-E_{ij}/kT)}}{U_j} \qquad (11.17)$$

The w_{ij} are the occupation probabilities of levels i in ionization state j. The occupation probabilities do not have a sharp cut-off, but approach zero for high-n as they are 'dissolved' due to plasma interactions. The partition function is redefined as

$$U_j = \sum_i g_{ij} w_{ij} e^{(-E_{ij}/kT)}. \qquad (11.18)$$

- Q-MHD (Nafyonov et al.) used in OP work but with ad hoc cut-off

  w = 0.001
- w depends on density
- Level population also depends on temperature via Boltzmann factor

Stark ionization in a plasma

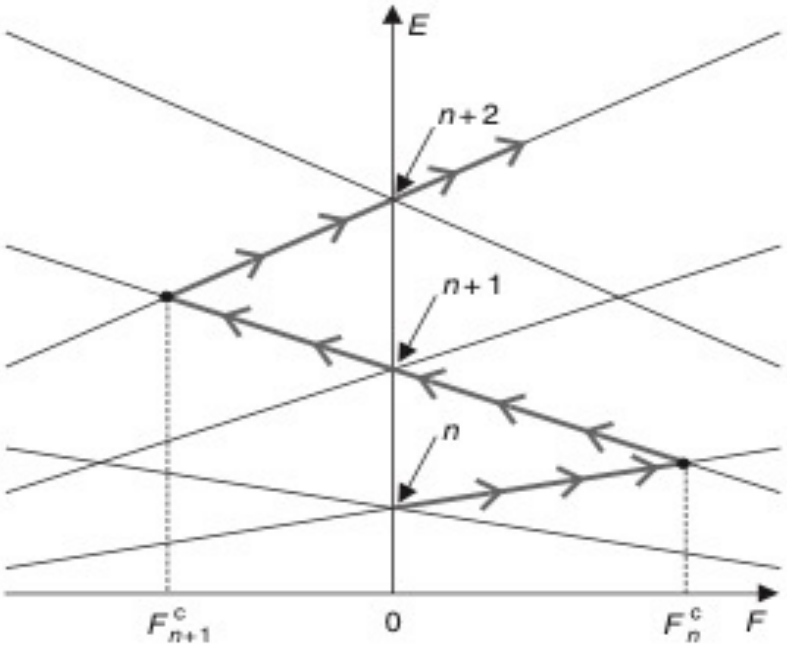

FIGURE 11.1 Stark manifolds of successive principal quantum numbers n, $(n+1)$, etc., showing level crossings among extreme states (adapted from [288]). The field strengths F^c_n, F^c_{n+1} are such that the manifolds n and $n+1$ intersect and the electrons move along arrows as shown.

How does one determine the occupation probability of a level in plasma environment?

1. Need to account for
   - electron-scattering
   - ion electric micro-field effects
2. Stark effect: energy levels split into sub-levels comprising a Stark n-manifol
3. The n-manifold width depends on field strength F and increases with n
4. At a critical field strength F_c , the highest sub-level of n will intersect with the lowest sublevel of n+1, and will be ionized as shown
5. F_c depends on temperature and density and yields the occupation probability w

MHD-EOS Level Populations

Table 3. MHD Equation-of-state parameters for Fe XVIII at solar BCZ: $T = 2 \times 10^6 K$, $N_e = 10^2 3cc$. Out of 1604 bound levels calculated, the lowest six levels, energies, occupation probabilities W(OP), and percentage level populations are given. The highest bound levels approaching the first ionization threshold $E \rightarrow 0$ are also given. The rapid decrease in W and N(%pop) by orders of magnitude is evident. Notation: 4.06(-5) = 4.06×10^{-5}.

Level	Energy (Ry)	W(OP)	N(% pop)
$1s^2 2s^2 2p^5 (^2P^o_{3/2})$	-99.924	1.00	8.79
$1s^2 2s^2 2p^5 (^2P^o_{1/2})$	-99.010	1.00	4.09
$1s^2 2s^2 2s (^1S_0)$	-90.156	1.00	2.03
$1s^2 2s^2 2p^4 3s (^4P_{5/2})$	-43.203	0.99	0.15
$1s^2 2s^2 2p^4 3s (^4P_{3/2})$	-42.957	0.99	0.05
$1s^2 2s^2 2p^4 3s (^4P_{1/2})$	-42.477	0.99	0.05
Highest levels $n > 4$	-0.500	0.56	4.06(-5)
Non-hydrogenic	-0.343	0.01	1.10(-7)

Fe XVIII at solar BCZ
T = 2×10^6 K, Ne = 10^{23} cc
W – Occupation Prob.
N(%) – Percentage Level Pop.

BCZ MHD-EOS Parameters: FeXVII

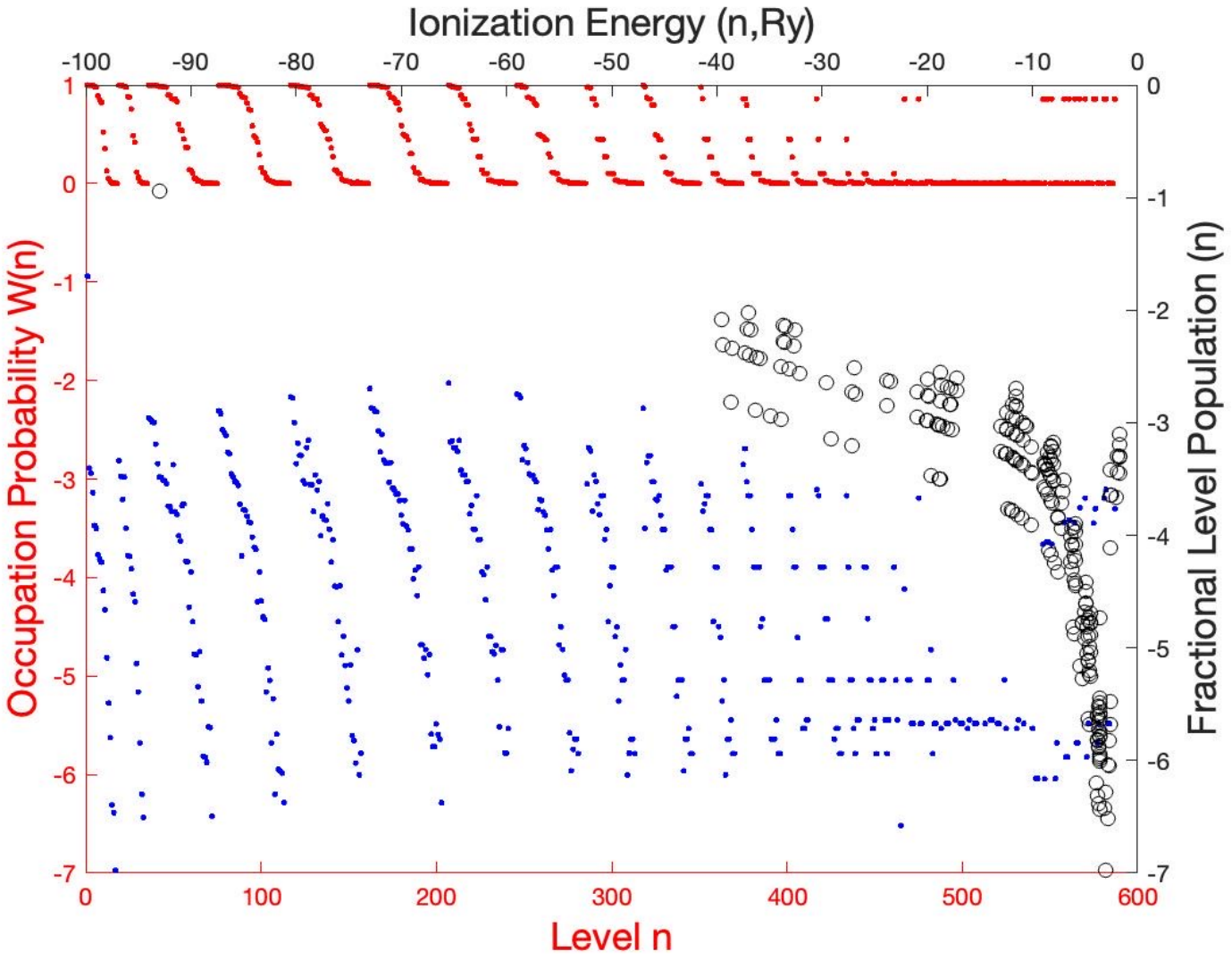

Convergence of RMO: Number of Levels in Iron Ions at BCZ and Z-Exp

- RMOs reach near-constant values at NLEV ~ 200
- R-matrix atomic datasets are over-complete
- NLEV = 454 (FeXVII), 1174 (FeXVIII), 1626 (FeXIX)
- Truncated by MHD-EOS
- No iron opacity contribution for NLEV > 200

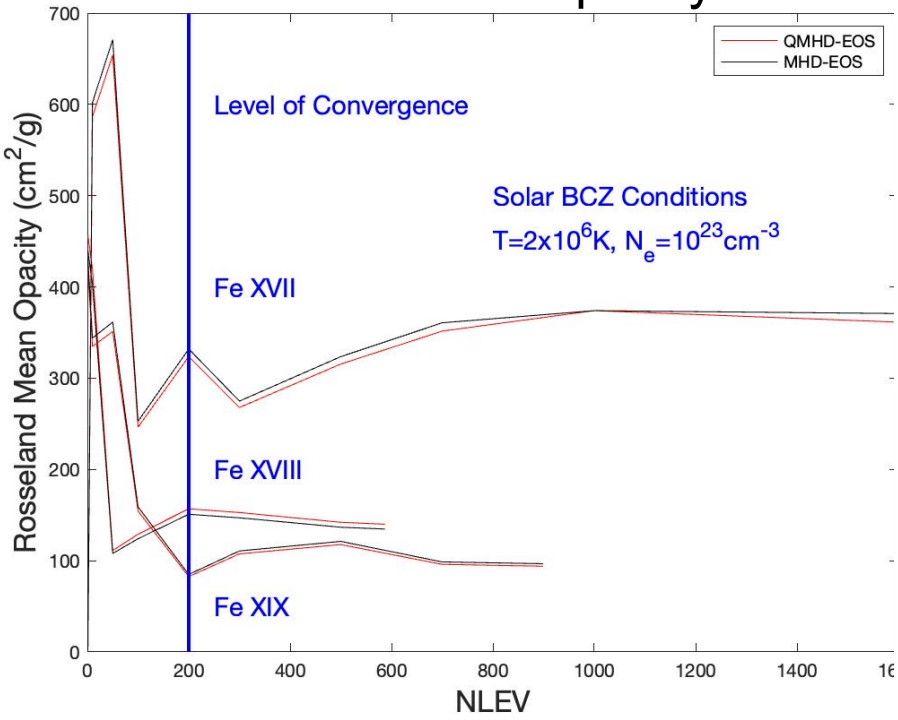

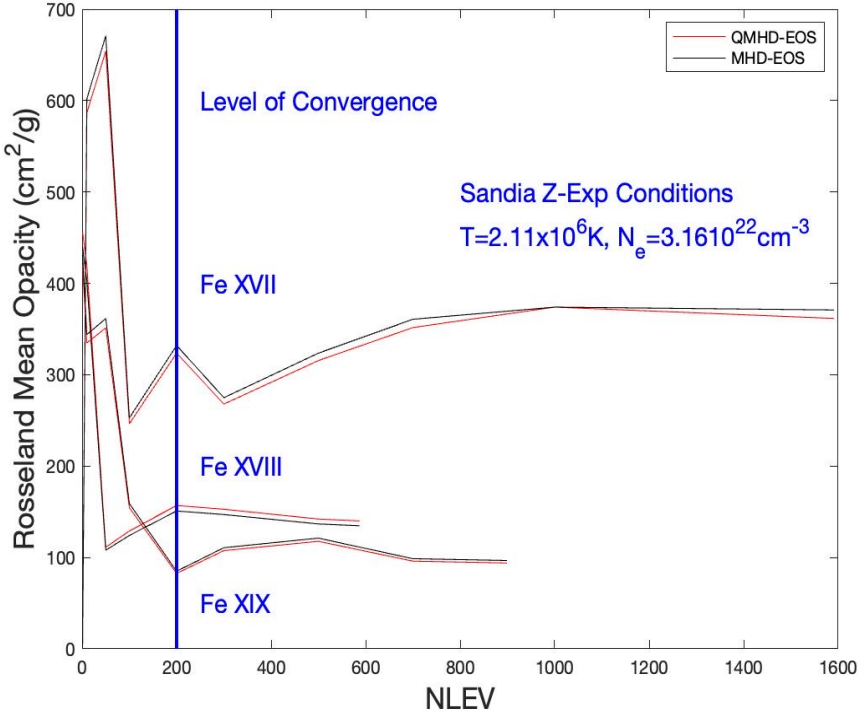

Monochromatic Iron Opacity Measurements (Sandia Z – Bailey et al., Nature 2015)

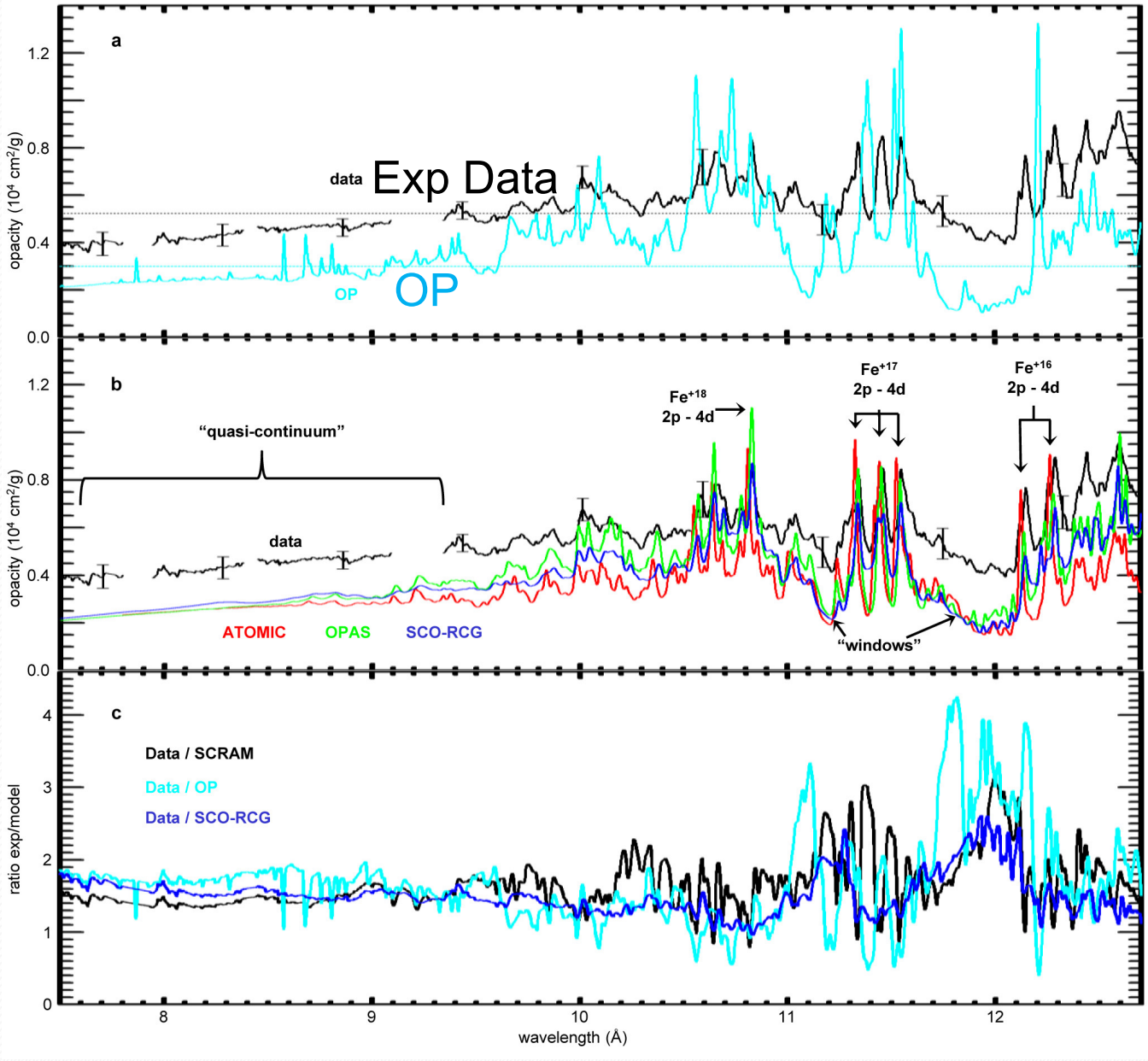

$T=2.1\times10^{6}$ K,
$N_e=3.1\times10^{22}$ cc

Z-energy range covers only part of the Rosseland window or the Planck function

Monochromatic Iron Opacity: OP, RMOP, Z-Experiment

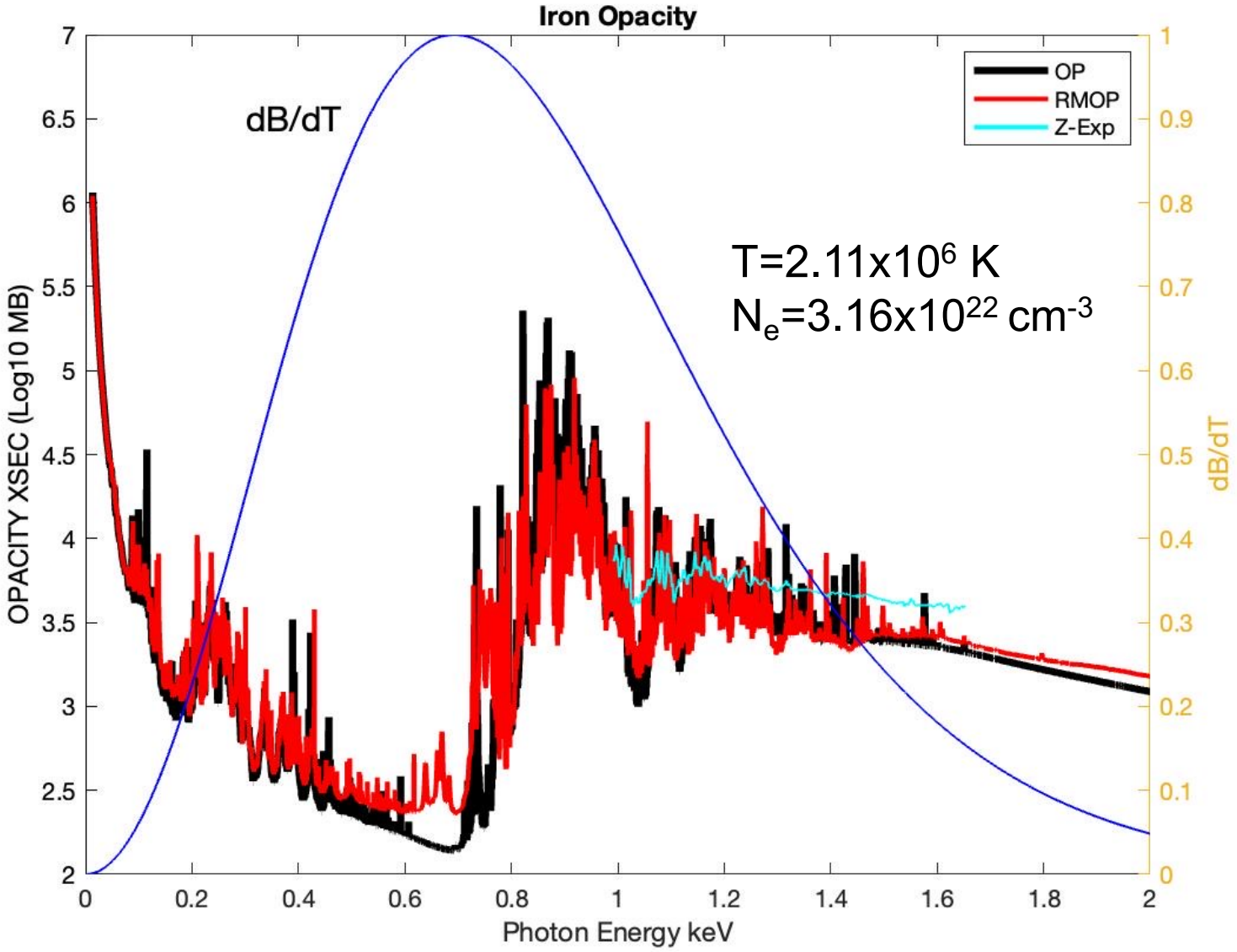

Plasma autoionization resonance broadening mechanisms

Total width = collisional + stark + doppler + free-free + core excn
Approximation → Normalized Lorentzian functional

$$\Gamma_i(\omega,\nu,T,N_e) = \Gamma_c(i,\nu,\nu_c)+\Gamma_s(\nu_i,\nu_s^*) + \Gamma_d(A,\omega)+\Gamma_f(f-f;\nu_i,\nu_i'), \quad (4)$$

Collisional:

$$\Gamma_c(i,\nu) = 5\left(\frac{\pi}{kT}\right)^{1/2} a_o^3 N_e G(T,z,\nu_i)(\nu_i^4/z^2), \quad (5)$$

Stark (N_e=N_p): F(MHD-EOS)

$$\Gamma_s(\nu_i,\nu_s^*) = [(4/3)\pi a_o^3 N_e]^{2/3}\nu_i^2. \quad (6)$$

Doppler (thermal) :

$$\Gamma_d(A,T,\omega) = 4.2858\times 10^{-7}\sqrt{(T/A)}, \quad (7)$$

Free-free opacity: transitions among Al levels E > 0 (~70,000 f-values for FeXVII)

Stark ionization parameter (MHD-EOS):

parameter $\nu_s^* = 1.2\times 10^3 N_e^{-2/15} z^{3/5}$ is introduced such

Plasma broadened cross sections of Fe XVII $2s^22p^5[^2P^o_{3/2}]3p(^3D_2)$ (ionization energy 37.707 Ry)

(Pradhan 2022)

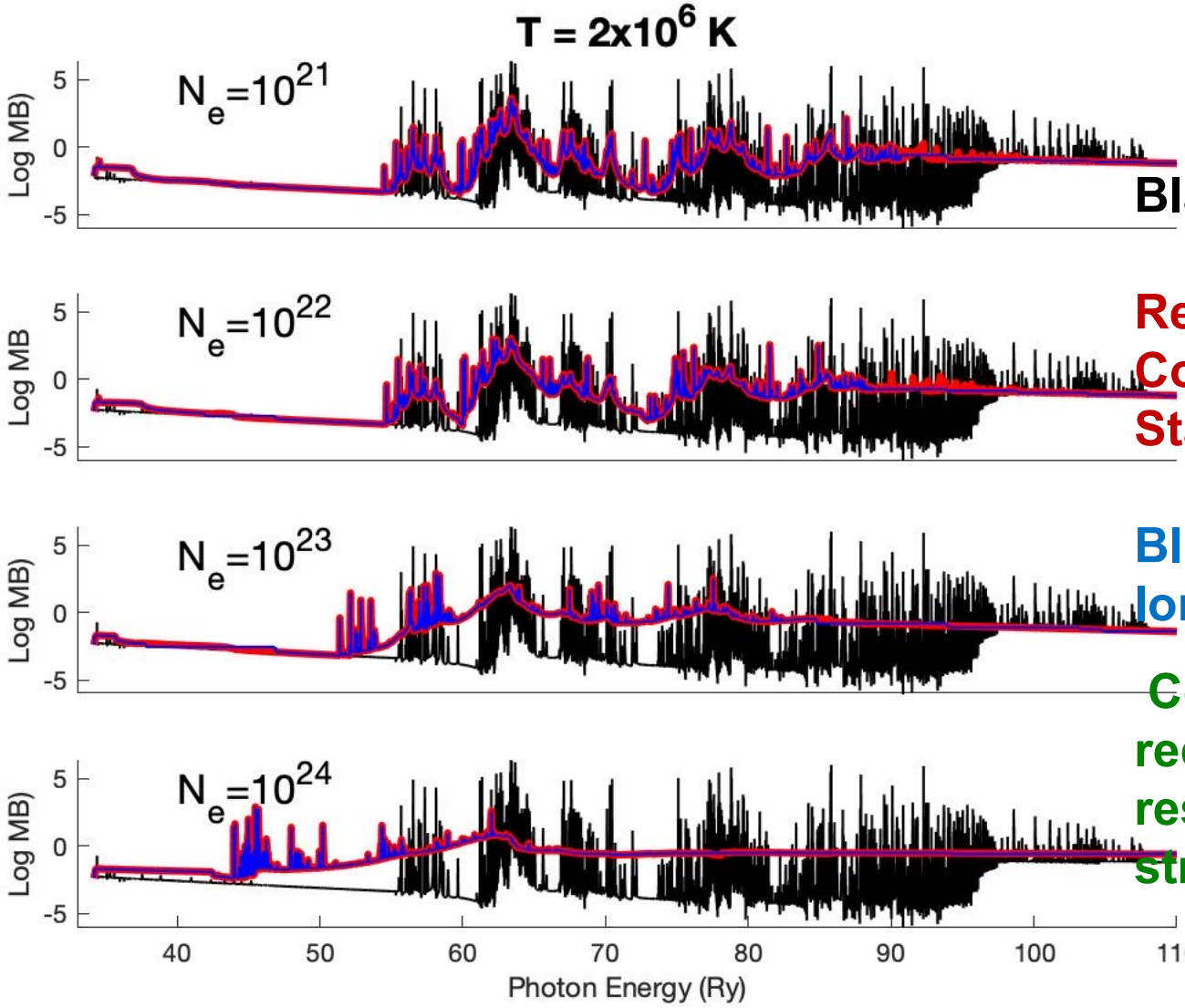

Black:Unbroadened

Red: Broadended – Coll. + Doppler + Stark + Core Excn.

Blue: With Stark Ionization cut-off

Considerable redistribution of resonance oscillator strengths

Plasma broadened cross sections of Fe XVII $2s^2 2p^5[^2P^o_{3/2}]4d(^1F^o_3)$ (ionization energy 17.626 Ry)

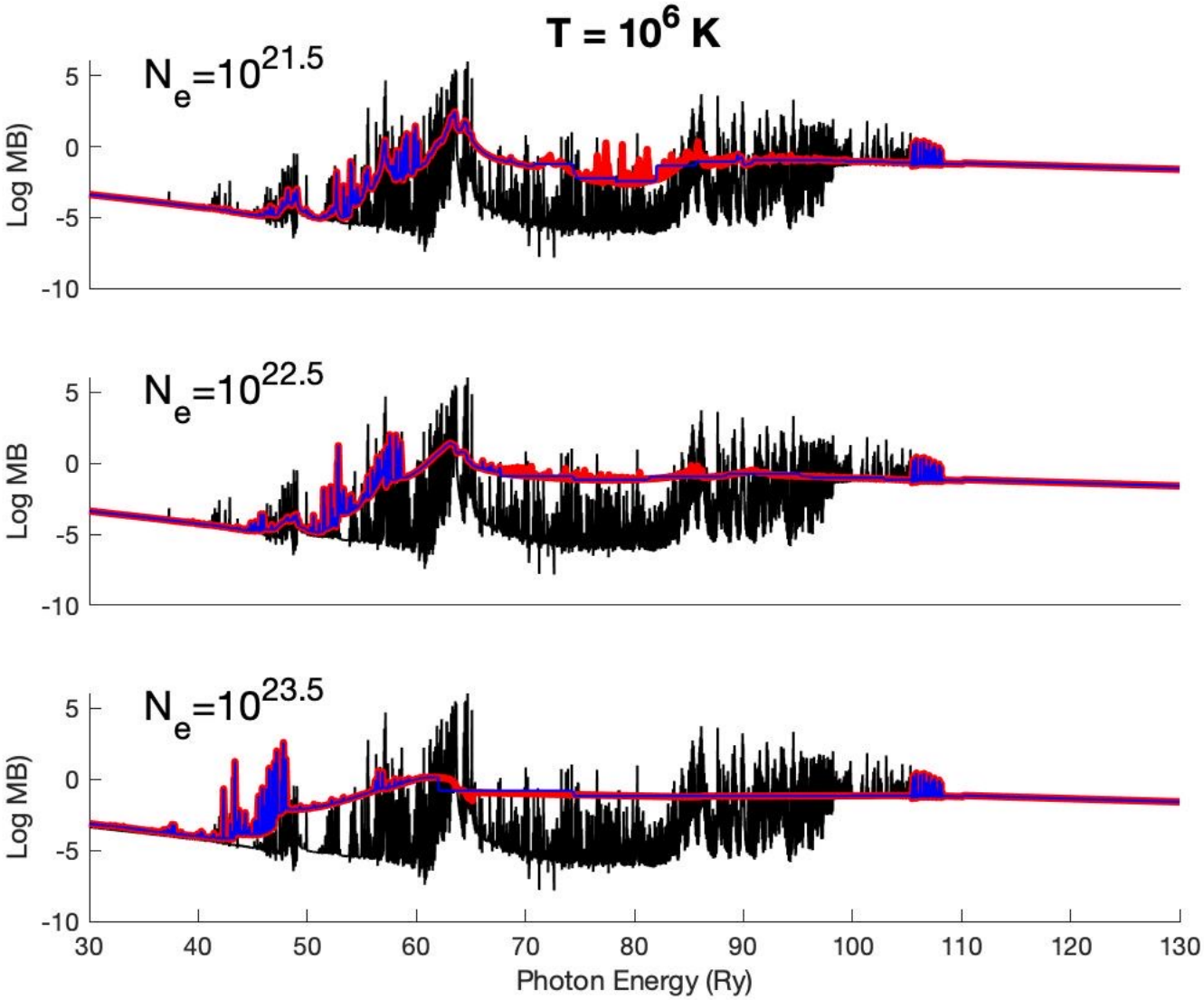

Table I: Plasma parameters along isotherms in Fig. 2 and 3; ν_D corresponds to Debye radius; R is the ratio of Fe XVII Rosseland Mean Opacity with and without broadening [23]; Γ_{10} is the maximum AI resonance width at $\nu = 10$.

T(K)	$N_e(cc)$	$\Gamma_{10}(Ry)$ $\nu = 10$	$\Gamma_c(10)$	$\Gamma_s(10)$	ν_s^*	ν_D	R
2×10^6	10^{21}	3.42(-1)	8.55(-2)	2.57(-1)	10.4	28.1	1.35
2×10^6	10^{22}	2.05(0)	8.55(-1)	1.19(0)	7.7	15.8	1.43
2×10^6	10^{23}	1.41(1)	8.55(0)	5.53(0)	5.6	8.9	1.55
2×10^6	10^{24}	1.11(2)	8.55(1)	2.57(1)	4.1	5.0	1.58
10^6	$3.1 \times 10^{21.5}$	8.17(-1)	2.71(-1)	5.46(-1)	9.0	17.8	1.47
10^6	$3.1 \times 10^{22.5}$	5.25(0)	2.71(0)	2.53(0)	6.6	10.0	1.13
10^6	$3.1 \times 10^{23.5}$	3.89(0)	2.71(1)	1.18(0)	4.8	5.6	1.06

Plasma Broadened and Unbroadened Cross Sections of Fe XVIII

$T = 2 \times 10^6 K$, $N_e = 3.16 \times 10^{22}$ cc

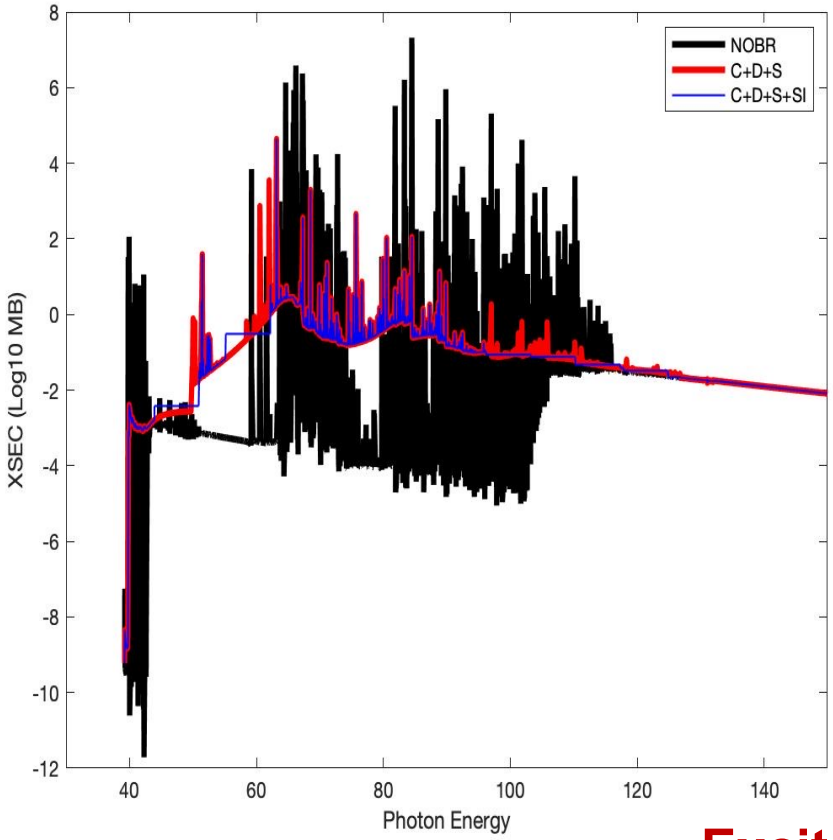

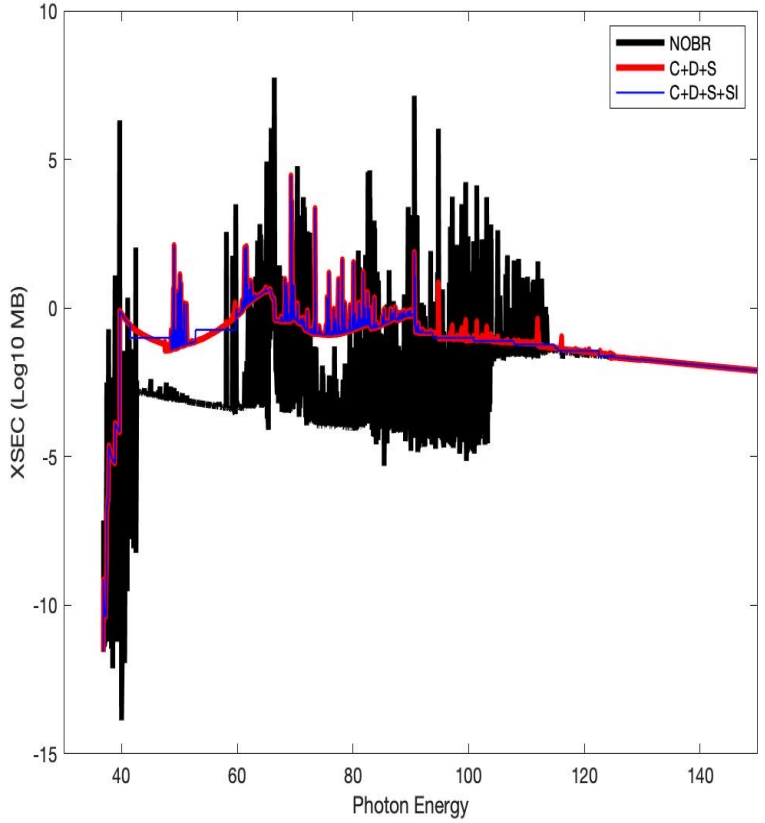

Excited levels

- Resonances and plasma broadening determines bound-free opacity
- BPRM cross sections for 1,174 levels of Fe XVIII, 454 levels of Fe XVII, 1601 levels of FeXIX

Fe XVIII Cross Section for same level on Log and Linear Scales

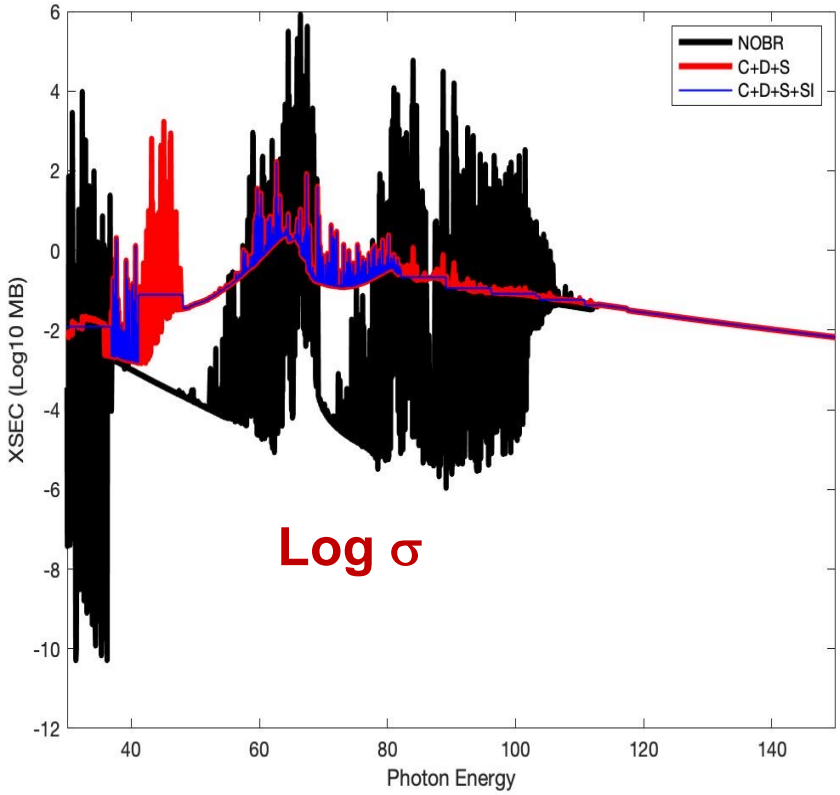

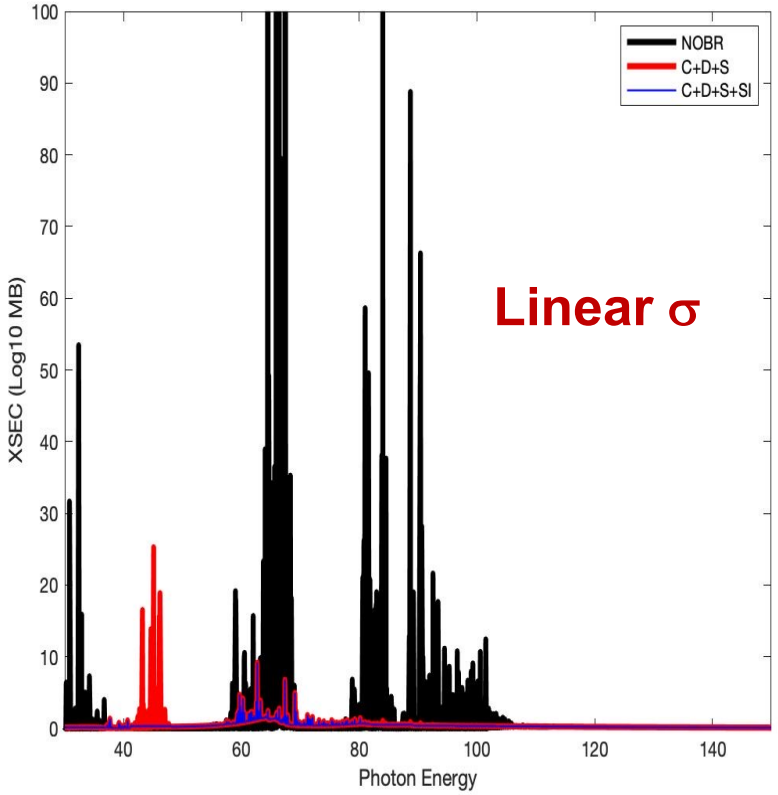

Plasma broadened opacity spectrum of FeXVII and Fe XVIII

$T = 2.11 \times 10^6 K$, $N_e = 3.16 \times 10^{22} cc$

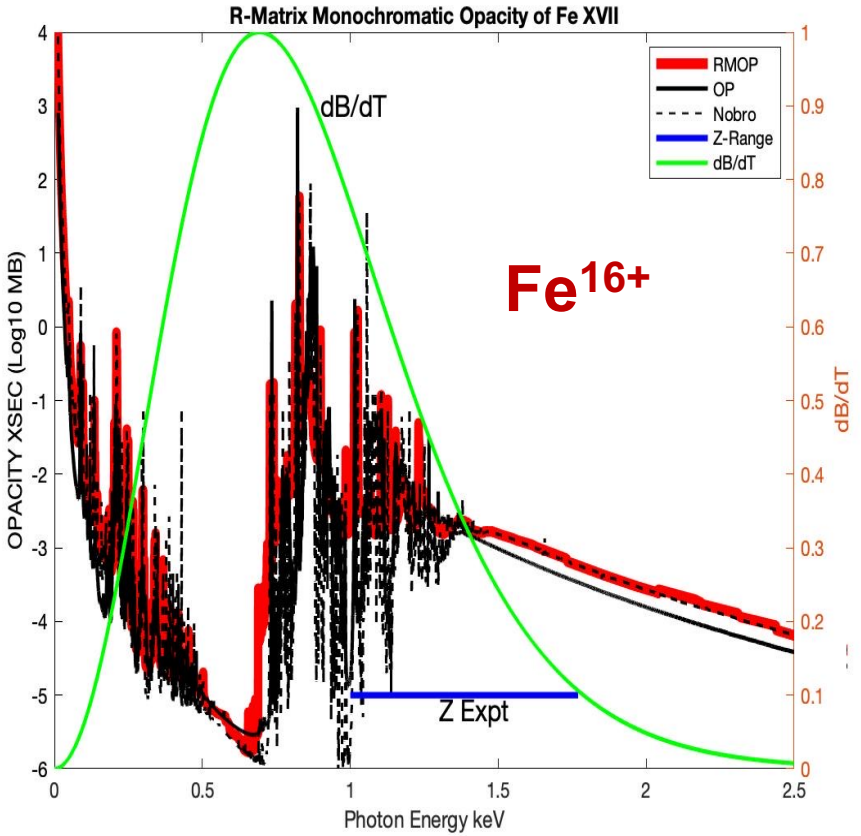

RMO: 1.35 x OP, 1.6 x Nobro

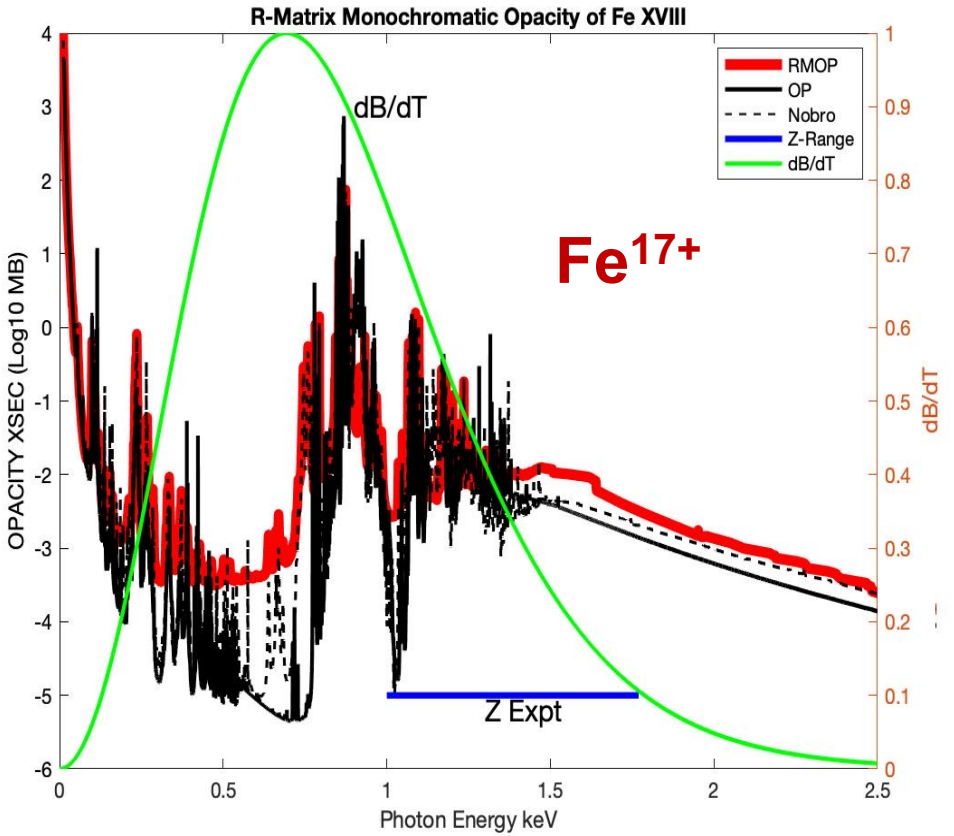

RMO: 3 x Nobro, 2 x OP

Fe vs. Cr, Ni Opacity Measurements (Sandia Z – Nagayama et al. 2019)

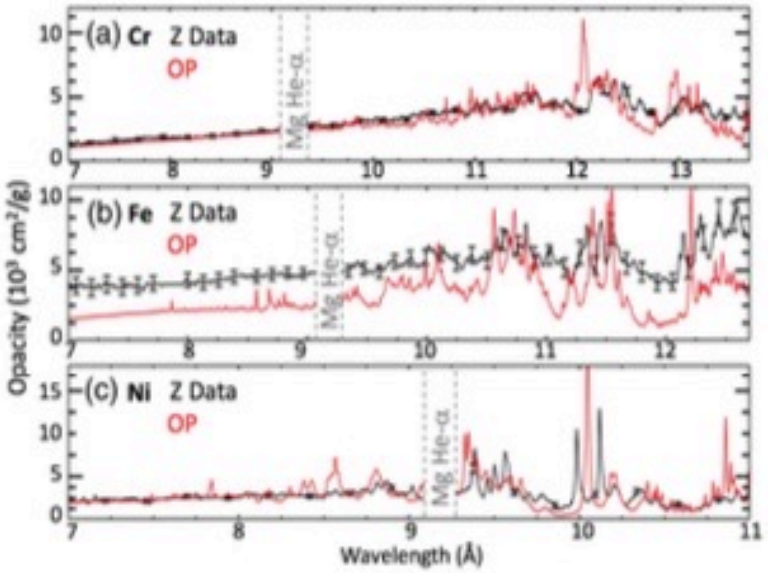

FIG. 3. Comparison of OP opacity (red line) and measured opacity (black line) approximately at 180 eV and 3×10^{22} cm^{-3} for (a) Cr, (b) Fe, and (c) Ni. Fe data and calculation are adopted from Fig. 3 of BNLR15. Opacities over 9.1–9.3 Å depend on the accuracy of Mg He-α removal and are not shown here. Wavelength upper limit is determined by the onset of strong lines from $n = 2 \rightarrow 3$ transitions, which are still under investigation.

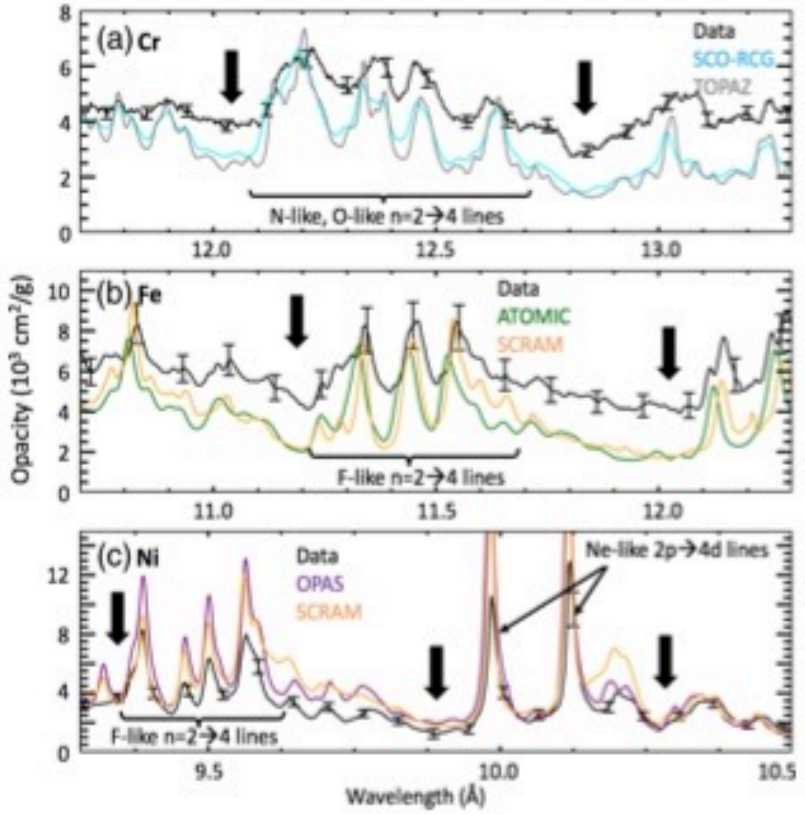

FIG. 4. Enlarged comparison of measured (black line) and modeled (colored lines) opacities for (a) Cr, (b) Fe, and (c) Ni

Enhanced Plasma Opacities: Opacity redistribution due to plasma effects

- **Intrinsic** autoionization broadening in RMOP calculations enhances extrinsic plasma broadening:
- Consistent with experiment: reduced peaks and windows in opacity spectrum compared to DW calculations
  resonances dissolve into continuum more rapidly than lines
- **RMOP Fe XVII-XIX RMOs are ~35-90% higher than OP**
  (BCZ conditions: $T=2\times10^6$ K, $Ne=10^{23}$ /cc
- RMOP opacity features agree qualitatively with experiment

(i) Plasma broadening fills in “windows”; redistributes opacity

(ii) Broadening significant for bound-free opacity for Ne $>10^{21}$/cc; increases with Ne

Conclusion and Future

- (Re-)newed R-matrix atomic and opacity codes
- Plasma effects on resonances in bound-free opacity
- RMOP iron opacities are higher
- Replace RMOP iron ion opacities in OP
- Equation-of-state issues
- Cr, Fe Ni (Sandia and Livermore experiments)
- O, Ne (Really?)
- Experiments at Sandia Z and Livermore NIF